Electrostatic interactions during activation of coagulation factor IX via the tissue factor pathway: effect of univalent salts

Maria P. McGee [a],*, Hoa Teuschler [a], Jie Liang [1,b]

[a] *Medicine Department, Rheumatology Section, Wake Forest University School of Medicine, Medical Center Blvd., Winston-Salem, NC 27157, USA*
[b] *Department of Biochemistry, College of Biological Sciences, 140 Gortner Laboratory, Gorter Avenue, St. Paul, MN 55108, USA*

Abstract

Interaction between the Gla-domain of coagulation proteins and negatively charged phospholipid membranes is essential for blood coagulation reactions. The interaction is calcium-dependent and mediated both by electrostatic and hydrophobic forces. This report focuses on the electrostatic component of factor IX activation via the extrinsic pathway. Effective charges during the reaction are measured by ionic titration of activity, according to the Debye–Huckel and Gouy–Chapman models. Rates of activation decrease with ionic strength independently of the type of monovalent salt used to control ionic strength. Moreover, the effect of ionic strength decreases at concentrations of charged phospholipid approaching saturation levels, indicating that membrane charges participate directly in the ionic interaction measured. The effective charge on calcium-bound factor IX during activation on phospholipid membranes is 0.95 ± 0.1. Possible sites mediating contacts between the Gla-domain and membranes are selected by geometrical criteria in several metal-bound Gla-domain structures. A pocket with a solvent opening-pore of area 24–38 Å^2 is found in the Gla-domain of factors IX, VII, and prothrombin. The pocket contains atoms with negative partial charges, including carboxylate oxygens from Gla residues, and has a volume of 57–114 Å^3, sufficient to accommodate additional calcium atoms. These studies demonstrate that electrostatic forces modify the activity coefficient of factor IX during functional interactions and suggest a conserved pocket motif as the contact site between the calcium-bound Gla-domain and charged membranes. © 1999 Elsevier Science B.V. All rights reserved.

1. Introduction

The vitamin K-dependent proteins that participate in blood coagulation are highly homologous at the N-terminal domain [1]. This domain is rich in γ-carboxyglutamic acid (Gla) residues and essential for binding interactions between coagulation proteins and negatively charged phospholipid membranes [2,3]. Evidence from X-ray crystallography supports the idea that bound calcium is required for maintaining the functional structure of the Gla-domain. Cal-

cium-free Gla-domains from various coagulation proteins invariably appear disordered, whereas all calcium-bound forms of the Gla-domain exhibit generally similar tertiary structure and are well defined [4–6].

On the basis of biochemical evidence, earlier models of Gla-domain interaction with charged membranes postulated the formation of several calcium bridges between the phospholipid head groups and Gla residues [7]. More recent proposals consider that calcium's role in membrane binding is secondary to its role in stabilizing the Gla-domain structure. This opinion is primarily based on analysis of atomic distances in calcium-bound prothrombin fragment 1 and, more recently, factor VIIa structures. In these structures most of the carboxylate oxygens of Gla residues overlap with calcium and do not appear to be available for additional calcium interactions [4]. Instead, a cluster of hydrophobic residues extending from the surface of the Gla-domain has been proposed as the primary site of interaction between Gla-domain and phospholipid membranes [8,9].

Several lines of biochemical evidence suggest that binding of Gla-domain to membranes requires direct, calcium-mediated ionic interactions. Higher numbers of calcium ions are associated with membrane-bound coagulation zymogens than with free zymogens in solution [10,11]. The affinity of coagulation zymogens for lipid membranes depends on the density of membrane charges [10–13]. Further, the affinity of calcium for the zymogen-membrane complex is about two orders of magnitude higher than the affinity of calcium for the membrane [14]. This latter observation suggests that there is a stereospecific component in the calcium-mediated interactions between zymogen and membrane.

Coagulation factors IX and X are vitamin K-dependent zymogens essential for hemostasis. The active forms of the proteases, factors IXa and Xa, are generated from the zymogens by specific proteolysis. The reaction is rapidly catalyzed by TF/FVIIa complexes [15,16]. Biologically relevant rates of zymogen activation by TF/FVIIa can be observed when the complex is assembled on negatively charged phospholipid membranes. This phospholipid requirement for fast substrate activation suggests that electrostatics play a direct role in the reaction, consistent with the observed ionic requirements for interaction

between the Gla-domain and the membrane. Recently, the activation of factor X both by intrinsic and extrinsic pathways has been reported to have an electrostatic component [17,18]. The possibility that factor IX activation reactions also have a significant electrostatic component has not been examined. From previous binding studies, it appears that factor IX has lower binding affinity for negative lipid membranes than factor X [11]. Structurally, the lipid-binding region of factor IX calcium-bound Gla-domain is localized to the 1–11 N-terminal residues [19].

In the present study, we analyze and compare the electrostatic component of factor IX activation reactions. Electrostatic interactions are analyzed by salt titrations on the basis of classical electrostatic theory [20–23]. Possible stereospecific site(s) for calcium-mediated contacts are investigated by analytical computational geometry, using the atomic coordinates of several Gla-domain structures in BH-PDB [24,25]. Our results demonstrate that electrostatic interactions play a significant role in the activation of factor IX, both in aqueous and membrane phase. The calcium-bound structures of factor IX and factor VII Gla-domain exhibit characteristic solvent-permeable pockets homologous to those previously described in strontium- and calcium-bound prothrombin structures [11,18]. This conserved three-dimensional motif may provide the structural basis for the specific calcium-dependent electrostatic interactions of coagulation zymogens.

2. Materials and methods

2.1. Preparation of tritium-labeled substrate

Sialic acid residues in factor IX were radiolabeled with tritium, using the general technique of Van Lenten and Ashwell [26], as adapted for human factor IX labeling [27]. This modification utilizes milder oxidation conditions than the original techniques, reducing the molar excess of $NaIO_4$ over protein sialic acid to twofold. The labeled preparation had specific activity of 4.6×10^8 CPM/mg and retained 92–98% of the biological activity in the original unlabeled preparation as determined by clotting tests with human plasma monodeficient in factor IX.

The TCA-soluble counts in the labeled preparation were 2.6% of the total, and on extensive activation, TCA-soluble counts leveled off at approximately 45–50% of the total.

2.2. Measurement of factor IX activation rate

Rate of factor IX activation to factor IXa by TF/FVIIa was measured, using an activation-peptide release assay as previously described [28], with minor modifications. Briefly, reaction mixtures contained TF, either naturally expressed on the cell or as recombinant human TF. Recombinant TF was either in solution or reconstituted into phospholipid vesicles. Other reactants were recombinant human factor VIIa and purified human factor H^3-IX (tritium-labeled factor IXa). Reactants were in Tris buffer (pH 7.2) with 2.5 mg/ml ovalbumin, 4 mM $CaCl_2$, and various concentrations of monovalent salts. Mixtures were in a total volume of 380 μl maintained at 32°C under constant stirring. Before initiation of reactions, mixtures were preincubated for 5 min to insure complete equilibration of the functional enzyme complexes formed by TF (essential cofactor) and factor VIIa (the enzyme component). Reactions were initiated by addition of the substrate factor H^3-IX, and samples, 30 μl each, were withdrawn at 0-, 10-, 15-, 20-, 30-, and 40-min intervals. For each sample, relative amounts of label not precipitated by 5% TCA were determined by scintillation counting. Reaction rates were determined by linear regression analysis of factor IXa concentration versus time data [25].

2.3. Coagulation factors

Recombinant human factor VIIa was a generous gift from Ulla Hedner (Novo Nordisk, Denmark). Full-length recombinant human tissue factor was purchased from American Diagnostics, Greenwich, CT. That the preparation includes the membrane-spanning region, was confirmed by amino acid sequencing analysis in the suppliers' laboratory. At the final dilution used in reaction mixtures, the preparation contained ∼0.0001% CHAPS (3-[(3-cholamidopropyl)dimethylamonio]-1-propanesulfonate) and ovalbumin at 2.5 mg/l. Recombinant tissue factor was incorporated into 30%/70% PS/PC as de-

scribed [29]. The functional activity of TF, in radiometric assays, increased over 100-fold upon relipidation on PSPC vesicles. The molar ratio of protein to phospholipid in the TF–PS/PC preparation was 1/4125 in the standard reaction mixtures used to determine effective charges. In some experiments, a 2–30-fold molar excess of 30%/70% PS/PC was added to the TF–PS/PC preparation. Human factors IX and X were from Enzyme Laboratories, South Bend, IN. Titrations of factor VIIa with aqueous phase TF were performed with factor VIIa chromogenic substrate, Spectrozyme (American Diagnostics), at 0.5 mM, pH 8.3.

2.4. Cells and cell culture

The human monocitoid cell line THP-1 was used to measure reaction rates on natural membranes. Cells were obtained from the American Type Culture Collection (Rockville, MD) and were maintained in suspension cultures as described before [18]. Expression of TF was induced by 3-h incubation with bacterial lipopolysaccharide (1 μg/ml) in serum-free medium supplemented with 2% low-protein serum replacement (Sigma Chemical Co., St. Louis, MO). Cell viability determined by Trypan Blue dye exclusion was >95%. For rate measurements, cells were washed and resuspended in reaction buffer containing 2.5 mg/ml ovalbumin. Final cell concentration in reaction mixtures was 1.5×10^6/ml corresponding to a total phospholipid concentration of 16 μM. At this cell concentration, factor IX activation rates were similar to rates measured with 0.1 nM TF-PSPC in radiometric assays.

2.5. Salt titration experiments and determination of effective electrostatic charge

The effect of ionic strength on factor IX activation was determined by measuring reaction rates at fixed concentrations of reactants while varying concentrations of monovalent salts from 0.1 to 0.3 M. As described earlier [16–20], by combining Debye–Huckel's expression for the activity coefficients of ions in water and Bronsted's general formula for reaction velocity, we have:

$$\log k = \log k_0 + Z\sqrt{I} \tag{1}$$

where k is the reaction rate, k_0 is the reaction rate under standard reference conditions, Z is the product of the effective charge on reactants, and I is the ionic strength. This equation predicts a linear relationship between $\log k$ and $\sqrt{I}$. The slope of the line approximates the product of the charges.

To model the electrostatic interaction between a positively charged substrate and a negatively charged surface, we also use the Heimburg and Marsh derivation [30,31]:

$$k/k' = I^{-(Z_s + AZ_s)} \cdot f^{2Z_s} \tag{2}$$

Here k is the apparent association rate constant for initial substrate–surface interaction, k' is the intrinsic binding constant, f is the fraction of binding surface that is charged, and Z_s is the charge on the substrate. The term in A includes several constants and has a negligible relative value for ligands with low effective charge [30]. Eq. 2 is derived by equating the change in electrostatic free energy during the interaction to the difference in the system's electrostatic free energy before and after the interaction. The electrostatic free energy of the surface is obtained on the basis of the Gouy–Chapman double-layer model; the electrostatic self-energy of the substrate is obtained on the basis of the Debye–Huckel model [30–33]. This derivation involves two assumptions about the nature of the reactive surface. First, the surface is negatively charged. Second, the negative charges are distributed homogeneously over the reactive surface. In principle, the model is applicable to any charged surface, including phospholipid membranes and polypeptide surfaces. Eq. 2 predicts a linear relationship between the natural logarithm, ln, of the initial rate and the ln of the ionic strength. The slope approximates the effective charge Z_s on the substrate before electrostatic neutralization, when the substrate is in the aqueous phase directly above the charged membrane [30].

The relationships in Eqs. 1 and 2 describe the general effect of ionic strength on the spatial distribution and, hence, the activity coefficient of reactants. They are valid at low, nonsaturating concentrations of reactants. Furthermore, these relationships are about overall electrostatic effects; the specific type of monovalent salt used to adjust the ionic strength should have no effect. The distribution of charged reactants is described by combining a Boltzmann ex-

ponential and classical electrostatic field theory [32], assuming simplified geometrical models for the interacting ions. This implies that although the experimental slopes reflect the magnitude of the participating charges, their absolute values may not correspond numerically with the total charges carried by reactants. The theory behind these derivations is very general and makes no assumptions about either the number of intermediate steps in the reaction or any other structural and mechanistic details [16–19,30–33].

2.6. Analysis of pocket structures in factor IX Gla-domain

The accessible pockets on the Gla-domains of several coagulation proteins are identified using the CAST program, which is based on the alpha shape and discrete flow theories from computational geometry. This software is available from the National Center of Supercomputing and its applications at the University of Illinois, Urbana-Champaign [20–23]. The atomic lineage, the volume, and area of the pockets as well as the area of the pocket openings are calculated using analytical formulae and atomic coordinates of structures deposited in BH-PDB. Theoretical and algorithmic background behind the alpha shape and discrete flow method have been described elsewhere [20–23].

For the analysis of pocket structures, the weighted Delaunay triangulation of atomic coordinates is computed using the program DELCX, where the convex hull of atom centers is obtained and then tiled with tetrahedra [21,22]. Delaunay triangulation provides the same information as the Voronoi diagram [23,34,35], which decomposes the space into non-overlapping Voronoi regions, each surrounding one atom. Inside these regions any point in space is closer to the assigned atom than to any other atom in the molecule. The weighted version of the Delaunay triangulation provides proper treatment for atoms of different radii. The alpha shape is derived from the Delaunay triangulation using the program MKALF, where geometrical information is further organized [22–24]. Surface pockets are located and measured using the program CAST and data from the Delaunay triangulation and alpha shape. These pockets are water-permeable, concave regions on the

protein that have one or more access openings to solvent space, where the area of the opening is smaller than one of the interior cross sections of the pocket. Once all surface pockets of the structure are identified and measured, likely candidates for stereospecific calcium binding sites are selected following two criteria: one, the pocket must have carboxylate oxygens from Gla residues lining its wall, and two, it must be large enough to accommodate at least one calcium atom.

We have analyzed the surface pockets of the Gla-domains of human factor IX (BH-PDB reference 1cfi, NMR structure), factor VIIa (1dan, X-ray structure), and prothrombin fragment 1 (2pf2 and 2pst, X-ray structures). For presentation, pockets identified and measured by analytical computational geometry are visualized in the structures with programs ALVIS and RASMOL.

3. Results

3.1. The effect of ionic strength on factor IX activation by tissue factor/factor VIIa

The activation rate of factor IX was measured at different levels of ionic strength with enzyme components assembled in solution, on phospholipid vesicles, or on live cell membranes. The concentration of monovalent salts was varied within the range of 0.1–0.3 M. For each set of rate measurements where ionic strength was adjusted, concentration of calcium and all other components was maintained constant. Calcium was at 4 mM, factor IX was at 45 nM, and factor VIIa at 4 nM. For reactions in aqueous phase, TF was at 15 nM. For reactions on artificial membranes, TF was added as a TF–PSPC vesicle suspension with TF protein concentrations of
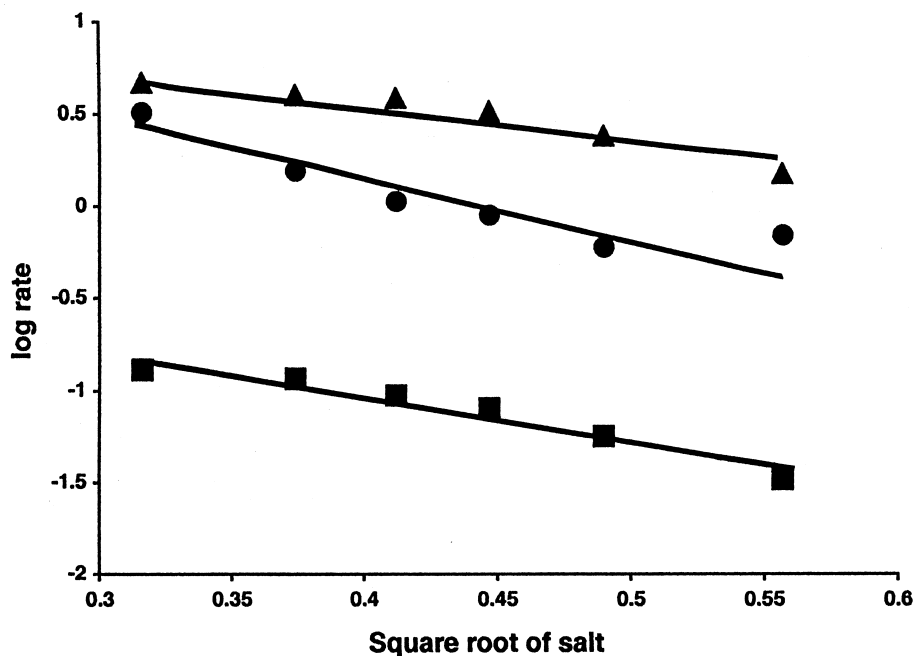

Fig. 1. Relationship between ionic strength and reaction rates. Rates of factor IX activation by the TF/factor VIIa complex are measured by radiometric assay. Ionic strength was fixed with NaCl at concentrations ranging from 0.1 to 0.3 M. The enzyme complex was assembled in aqueous phase (■) with TF and factor VIIa at 15 and 4 nM, respectively, on PSPC (30%/70%) membranes (▲) with TF and factor VIIa at 0.1 and 4 nM, respectively and, on THP-1 cells at 1.5×10^6/ml (●) with factor VIIa at 4 nM. The concentration of functional TF in mixtures with THP-1 cells is estimated at ~0.1 nM, using TF–PSPC as reference. Reactions are initiated with ^{3}H-factor IX at 45 nM. The log of normalized reaction rates (nM FIXa/TF-VIIa/min) is plotted versus the square root of ionic strength according to Eq. 1. The equation is fitted to data points by least squares, linear regression method [38]. Coefficients of determination, R^2, for the regression lines are > 0.9.

0.1 nM. For reaction on natural membranes, THP-1 cell suspensions were adjusted to a concentration of 1.5×10^6/ml, resulting in reaction rates similar to rates measured with 0.1nM TF–PSPC and 15 nM aqueous-phase TF.

The reaction rate decreases with ionic strength (Fig. 1). Results from both aqueous-phase and membrane reactions under varying ionic strength demonstrate that the change in the rate of factor IX activation with ionic strength followed the relationships predicted by Eqs. 1 and 2: Plots of the log of reaction rates versus the square root of ionic strength were linear; plots of ln of reaction rates versus ln of ionic strength were also linear. These linear relationships were valid for several types of monovalent salts. The negative slope is consistent with interaction between reactants with electrostatic charges of opposite signs [20–23,30–33,36]. Table 1 lists the product of the charges of the reactants as determined from Eq. 1 and the charge of factor IX as determined from Eq. 2. It includes data from both aqueous solution and PSPC membrane systems.

3.2. Effect of ionic strength at different reactant concentrations

The predictions of Eqs. 1 and 2 are based on changes in the activity coefficient of reactants with ionic strength. Therefore, the electrostatic charges detected are only for those reactants whose concentration is directly proportional to reaction rates. To identify the reactants that contribute to the product of charges measured, the effect of ionic strength is analyzed at various reactant concentrations. First,

we test enzyme-complex and substrate concentrations. In these experiments, factor IX is at 18–90 nM, TF/PSPC at 0.02–0.4 nM, and factor VIIa at 4 nM, saturating for TF/PSPC. For aqueous phase reactions, TF is at 3–15 nM and factor VIIa at 4 nM. Monovalent salts are varied within the range of 0.1–0.3 M. Within this experimental range of ionic strengths and reactant concentrations, the rate of factor IX activation is found proportional to the concentration of both the enzyme-complex and the substrate. Figs. 2 and 3 show results for reactions on PSPC vesicles. Similar results are obtained with aqueous-phase reactions. These findings demonstrate that under these experimental conditions, the effect of increased ionic strength is reflected in the lower activity coefficient of these reactants.

To determine the component charge detected in membrane reactions, measurements are repeated in mixtures containing a fixed concentration of TF/VIIa–PSPC and increasing concentrations of either PSPC or PC. Results of these titrations with phospholipid are shown in Fig. 4A. At standard physiologic ionic strength, reaction rates increase with PSPC concentration but not with PC. The rate increases observed with PSPC approach asymptotically to a maximum. The $K_{1/2}$ (concentration of added PSPC resulting in half-maximal reaction rates, estimated by fitting rectangular hyperbolas to data points) is 6.4 ± 1.2 μM of PSPC and equivalent to 1.8 μM of PS.

Results from salt titrations of reaction mixtures with PSPC at concentrations 2.5-fold above $K_{1/2}$ are plotted in Fig. 4B. The value of the slope of log rate versus square root of ionic strength is sig-

Table 1
Effective charges during factor IX activation in the presence of different anions and cations

Salt	Product of charges		Charge on factor IX	
	aqueous	PSPC	aqueous	PSPC
NaCl	2.10 ± 0.22	1.80 ± 0.25	1.20 ± 0.13	0.86 ± 0.16
CsCl	2.28 ± 0.24	2.35 ± 0.18	1.10 ± 0.14	1.15 ± 0.08
NaBr	2.09 ± 0.20	2.45 ± 0.38	0.99 ± 0.09	1.16 ± 0.23
NaI	2.22 ± 0.21	2.50 ± 0.19	1.09 ± 0.10	1.21 ± 0.16

Reaction rates were measured at ionic strengths ranging from 0.1 to 0.3, maintained with the various monovalent salts indicated. The product of the charges on reactants and the charges on factor IX are determined from Eq. 1 and Eq. 2, respectively. Charge values obtained with a specific salt do not significantly differ from the overall average values. The average values are 2.17 ± 0.093 and 2.27 ± 0.32 for the charge product in aqueous and PSPC reactions, and 1.1 ± 0.086 and 1.1 ± 0.16 for the charge on factor IX in aqueous and PSPC reactions, respectively.
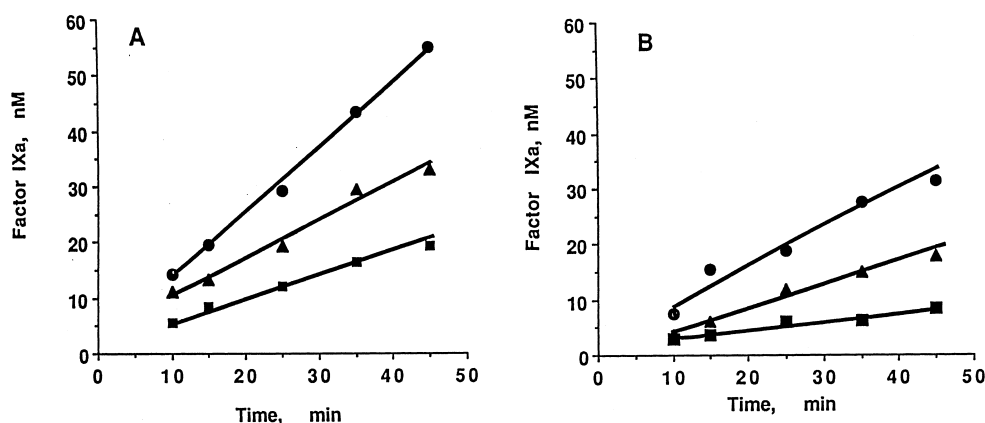
Fig. 2. Reaction rates at different ionic strength and substrate concentrations. Rate of factor IX activation by TF/factor VIIa is measured by radiometric assay. Ionic strength is fixed with NaCl, with CaCl$_2$ maintained at 4 mM. Reaction mixtures contain TF–PSPC, 0.1 nM; FVIIa, 4 nM; and 5 mg/ml ovalbumin in Tris buffer at pH 7.2. Data is from reactions measured at ionic strength of 0.1 (panel A) and 0.25 (panel B). Reactions are initiated with radiolabeled human factor IX at 180 (●), 90 (▲) and 45 nM (■). Factor IXa concentration is determined from TCA-soluble counts in samples taken at time intervals in the abscissa. Reaction rates determined from the slope of lines fitted to data points by linear regression were 1.21 ± 0.03 (●), 0.73 ± 0.05 (▲), 0.43 ± 0.02 (■) nM/min in panel A and 0.74 ± 0.06 (●), 0.41 ± 0.02 (▲), 0.17 ± 0.02 (■) nM/min in panel B. Similar results were obtained for reactions in aqueous phase (not shown).

nificantly lower for reaction mixtures with 16 μM PSPC than for those with 0.8 μM PSPC.

In contrast to reactions on TF/PSPC vesicles, rates on cell membranes do not increase significantly with added PSPC. Reaction rates measured at physiologic ionic strength, 0.15, with added PSPC at 160, 106, 47, 32, and 21 μM are 0.26 ± 0.02, 0.27 ± 0.02, 0.28 ± 0.03, 0.29 ± 0.01, and 0.25 ± 0.01 nM factor IXa/min, respectively. Therefore, at physiologic ionic

strength and similar TF activity level, added PSPC modifies the substrate's activity coefficient more efficiently on TF–PSPC than on cell suspensions. However, at higher ionic strength, PSPC vesicles also increase rates of reactions on cell membranes (and decrease the slope of Eq. 1). Salt titrations with added PSPC at 0, 16, 32, and 64 μM give slopes of −2.6 ± 0.56, −2.5 ± 0.32, −1.8 ± 0.58, and −1.3 ± 0.41, respectively.
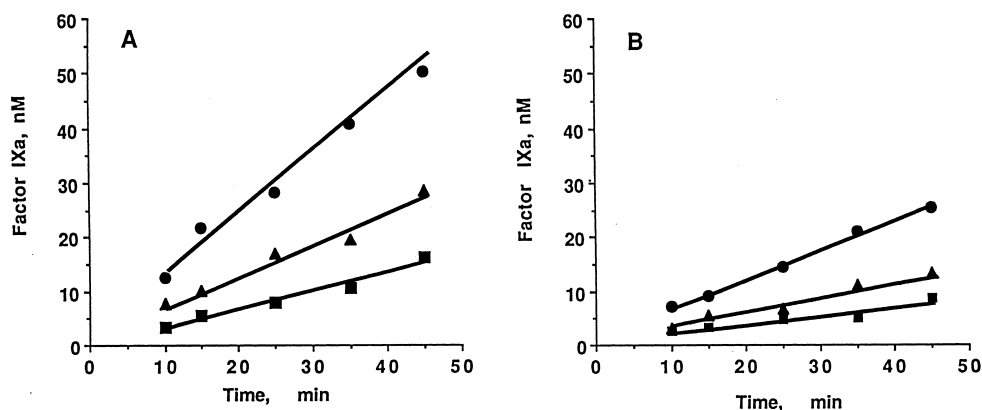

Fig. 3. Reaction rates at different ionic strengths and enzyme/cofactor complex concentrations. Reaction mixtures were as indicated in Fig. 1 except that factor IX was at 45 nM, while TF (as TF–PSPC) was at 0.2 (●), 0.1 (▲) and 0.05 (■) nM. Data is from reactions measured at ionic strength of 0.1 (panel A) and 0.25 (panel B). Reaction rates determined from the slope of lines fitted to data points by linear regression were 1.2 ± 0.05 (●), 0.596 ± 0.04 (▲) and 0.34 ± 0.02 (■) nM/min and 0.56 ± 0.02 (●), 0.29 ± 0.02 (▲), and 0.17 ± 0.02 (■) nM/min, respectively. Similar results were obtained for reactions in aqueous phase (results not shown).
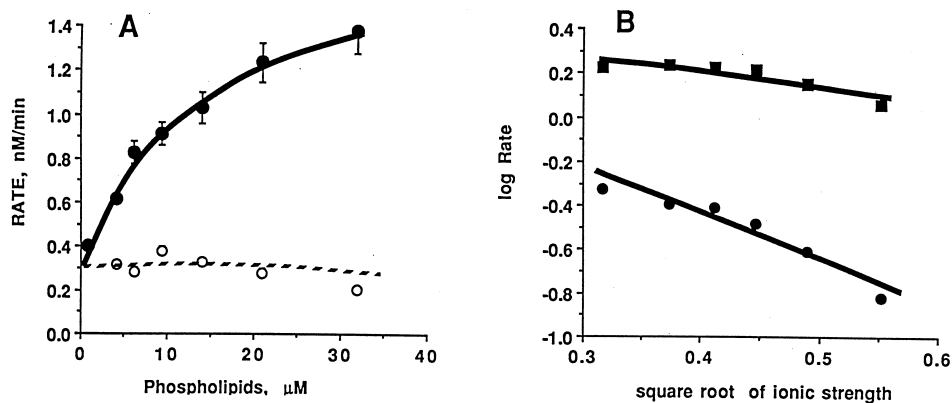
Fig. 4. Effect of ionic strength at different lipid concentrations. (A) Reaction rates are measured in the presence of added phospholipid either PS/PC (●) or PC (○), at concentrations indicated in the abscissa. Ionic strength was fixed at 0.15, TF/PSPC was at 0.1 nM TF, 0.8 μM PSPC. Other reagents were as indicated in Fig. 1. Data points and error bars are initial rates determined from product versus time curves as in Fig. 1. Concentration of added PSPC giving half-maximal rates, estimated by fitting a rectangular hyperbola to data points, is 6.4 ± 1.1 mM (mean $\pm$ S.D. from three independent titrations with PSPC). (B) Reaction rates are measured at different ionic strength levels in mixtures with 0.1 nM TF and either 0.8 (●) or 16 (■) μM PSPC. Other reagents are as in Fig. 1. The log of reaction rates (nM FIXa/min) is plotted versus the square root of ionic strength controlled with NaCl. The slope of fitted lines is -2.04 ± 0.29 and 0.70 ± 0.19 for reactions with PSPC at 0.8 and 16 μM, respectively.

Results with reactions on membranes (either natural or synthetic) and added PSPC are as predicted theoretically for electrostatic interaction between substrate and lipid charges.

Free calcium at the concentration required for optimal functional activity of coagulation enzymes and substrates may also contribute to the measured effective charges. To test this possibility, a series of measurements are made with calcium adjusted to 1, 2, 3, 4, 6, and 8 mM concentration and NaCl at either 0.1 or 0.25 M concentration. Under these conditions, the effect of ionic strength on reaction rates is found to be independent of free calcium concentration (Fig. 5). This demonstrates that the 4 mM level of free calcium is at saturation levels and thus, the effects of ionic strength on its activity coefficient do not translate into changes in the reaction rate. Therefore, if the positive electrostatic charges measured are from calcium, these charges are on calcium bound to substrate rather than on free calcium. (The possibility that the negative charges are on the substrate and the positive charges are from membrane-bound calcium is also excluded by the results. The binding constant between calcium and PSPC membranes is 12 M^{-1} [14] and therefore not saturated at the mM concentrations used.)

3.3. Pocket structure of the Gla-domain of factor IX

Results from salt titrations are fully consistent with electrostatic interaction between calcium-bound substrate and negative charges on the membrane. Quantitatively, the interaction involves few effective
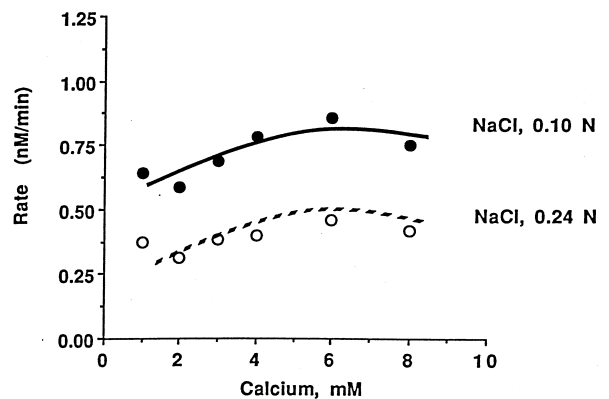
Fig. 5. Effect of ionic strength at different calcium concentrations. Reaction rates, expressed as nM factor IXa/min in the ordinate, are measured at the same reactant concentrations indicated in Fig. 1. Factor IXa is fixed at 90 nM. Calcium concentration is varied as indicated in the abscissa. The ionic strength is maintained at either 0.1 (●) or 0.24 (○) with NaCl. Data is for reactions in PSPC membranes. Similar results are obtained for reactions in aqueous phase (not shown).

charges, with 1–2 positive charges on the substrate. If calcium bound to substrate is providing all or part of these positive effective charges, the calcium interaction with the substrate must be stabilized by stereo-specific determinants. This follows from the fact that the affinity of calcium for substrate is higher than that expected for simple electrostatic attraction. Therefore, the calcium atoms mediating the interaction between substrate and membrane must be both exposed to solvent and stabilized by shape determinants in the protein. These two conditions are fulfilled in the binding pockets of proteins.

The structure used to search for calcium-binding pockets in factor IXa is that of a synthetic peptide, consisting of the 47 N-terminal residues, determined from NMR data [5]. This Gla-domain structure is calcium-bound, although the calcium atoms are not resolved. The structure of surface pockets, including location, atomic composition, and metric parameters, was characterized using the alpha-shape method of computational geometry. This procedure is analytical, can handle atomic overlaps of more than four

atoms, and deals with degeneracy without changing the input. Fig. 6A shows a pronounced pocket in the Gla-domain region of factor IX, with an opening leading toward the bulk solvent environment. The volume of this pocket is 111.4 $Å^3$, and the area of its opening is 24.5 $Å^2$. Many of the atoms lining the pocket have negative partial charges (Table 2).

In addition to factor IX, calcium-bound structures of the Gla-domain of prothrombin fragment 1 (2pf2), strontium-bound prothrombin fragment 1 (2pst), and calcium-bound factor VII (1dan) have been solved [2,6]. The analysis in these structures shows that each has a large pocket in the Gla-domain, and all are homologous to the C pocket seen on prothrombin and factor IX (Fig. 6C,D,E). These pockets vary slightly in size (Table 3). Although the pocket atoms are not identical, they essentially involve the same set of amino acid residues (Table 2), after residue number is corrected according to sequence alignment. For the X-ray structures, the thermal fluctuations (as reflected by the B factor) are all within reasonable range.

Table 2
Atoms lining the conserved C pocket in the Gla-domain[a]

Ca^{2+}-Factor IX		Ca^{2+}-Factor VII		Ca^{2+}-Prothrombin		Sr^{2+}-Prothrombin	
CGU 7:	O	CGU 6:	OE2	CGU 7:	O	CGU 7:	O
	OE4	CGU 7:	O	CGU 8:	CA	CGU 8:	CA
	C		CD1		CD2		CD1
CGU 8:	O		OE1		OE4		OE1
	OE1		OE2		O		O
	CA	Arg 9:	O	Arg 10:	O		CB
Val 10:	CB	Gly 11:	CA	Gly 12:	N		C
	CG1		N		CA	Arg 10:	O
	CG2	Arg 15:	NH2	CGU 30:	CB	Gly 12:	N
Gly 12:	CA	CGU 16:	OE3		CD2		CA
Asn 13:	CB		OE4		OE2	Arg 16:	NH1
	N	CGU 26:	O		OE4	CGU 17:	OE1
	OD1	CGU 29:	OE2				OE2
Arg 16:	CD		OE4			CGU 27:	OE1
CGU 17:	OE1		CB			CGU 30:	CB
	OE4						OE4
CGU 27:	OE1						OE2
	OE2						O
CGU 30:	CB						
	OE3						
Ala 1:	CB						
Val 31:	CG2						

[a]The C pocket structure of Ca-bound factor IX Gla-domain is analyzed using the atomic coordinates in the NMR-determined structure (1cfi), BH-PDB. The same pocket structure on Ca-bound factor VII and Ca and Sr-bound prothrombin fragment 1 are analyzed from the atomic coordinates of X-ray crystal structures (files 1dan, 2pf2 and 2pst, respectively).
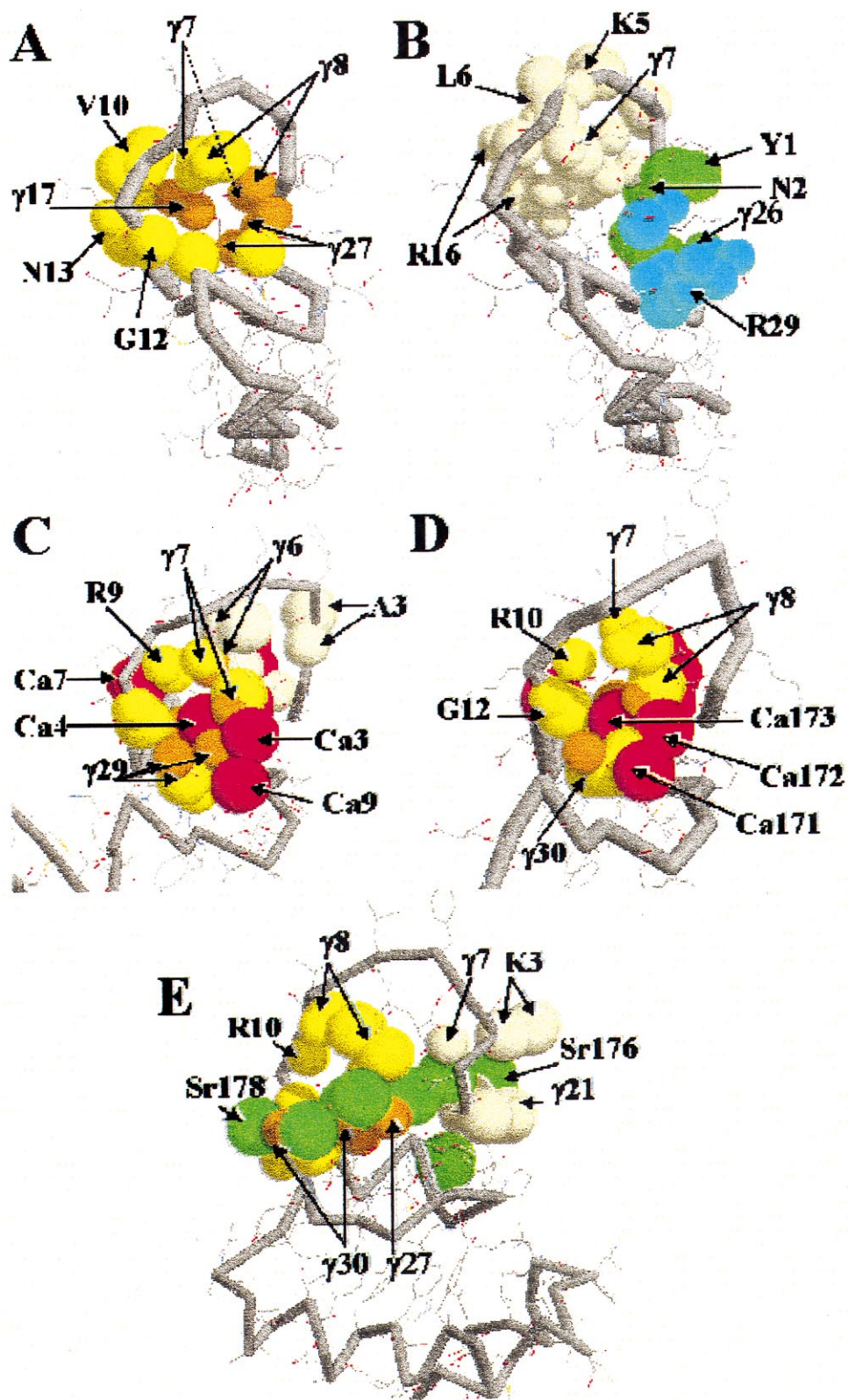
For factor IX, there is another, larger, adjacent pocket on the Gla-domain (pocket D, Fig. 6B). Pockets homologous to this pocket are also seen in calcium-bound factor VII (Fig. 6C) and strontium-bound prothrombin (Fig. 6E) but are absent from calcium-bound prothrombin. The volume and opening area of these D pockets are listed in Table 4 and their atoms in Table 5. The volume of pocket D in the X-ray (but not in the factor IX-NMR) structures is smaller than the volume of the calcium atom (~ 22 Å^3). In addition, two more pockets are found (Fig. 6B) on the Gla-domain of factor IX with volumes of 40.2 and 34.9 Å^3 and opening areas of 18.1 and 15.7 Å^2, respectively. These pockets do not have corresponding homologous pockets on the X-ray structures.

4. Discussion

We have measured the rate of factor IX activation by TF/FVIIa in both aqueous solution and on phospholipid membranes under varying ionic strength conditions. The results demonstrate that the rate depends on the ionic strength of the reaction environment for both aqueous and membrane systems. The effect of ionic strength follows theoretical predictions for interactions between charged reactants and for interactions between charged surfaces and charged substrates. Together with biochemical evidence, where calcium and Gla-domain are shown to mediate the binding of coagulation zymogens to membranes [1,10,12], these results indicate that there are direct electrostatic interactions between Gla-domain and phospholipid during the rapid activation of factor IX by TF/VIIa assembled on PSPC vesicles. The interaction is mediated by a net positive charge in factor IX and approximately two negative charges on the membrane. Charges on PS participate directly in the interaction on PSPC as demonstrated by the predicted decreased effect of ionic strength at high concentrations of PS. On natural membranes, added PSPC also decreases the effect of ionic strength, although less efficiently than on purified PSPC vesicles. This lower efficiency suggests qualitative differences between factor IXa interaction sites on artificial vesicles and on natural membranes. Similar

Table 3
Atoms lining pocket D in the Gla-domain structures[a]

Ca^{2+}-Factor IX		Ca^{2+}-Factor VIIa		Sr^{2+}-Prothrombin	
Tyr 1:	O	Ala 3:	CB	Lys 3:	CB
Ser 3:	CB		N		CD
	OG		O	CGU 7:	OE2
Lys 5:	CB	CGU 6:	OE1	CGU 21:	OE3
	CE		OE4		OE2
Leu 6:	N		CD2		OE4
	C		CB		CD1
	O	CGU 20:	OE3		
	CB				
CGU 7:	CA				
	CB				
	OE1				
	OE3				
Val 10:	CG2				
Arg 16:	O				
	CG				
	CD				
	NH2				
	OE1				
	OE2				
	CD2				
	OE3				
	OE4				

[a]Atoms forming the small pocket identified in 1cfi, 1dan, and 2pst.

←
Fig. 6. Pocket motifs in the Gla-domain of factors IX, VII, and prothrombin. Atoms lining the pockets are represented in space-filling balls superimposed on the backbone. These atoms are listed in Tables 2 and 3. (A) Calcium-bound factor IX, NMR structure of 1–47 N-terminal residues. (B) The same structure showing the D pocket in off-white, and the E and F pockets in green and blue, respectively. (These two pockets do not exist in the other structures.) (C) Calcium-bound factor VII, X-ray structure; only the Gla-domain and adjacent regions are included. (D) Calcium-bound prothrombin fragment 1, X-ray structure. (This structure has two additional and unique pockets in the Gla-domain. They were described previously [18] and are not shown here.) (E) Strontium-bound prothrombin fragment 1, X-ray structure. Atoms forming the C pocket in all four structures are yellow; atoms forming the D pocket in Ca-bound factor IX, VII, and Sr-bound prothrombin are off-white. Carboxylate oxygen atoms exposed to solvent in the C pocket are orange. Also, in pocket C, the calciums are in red and the strontiums in green. The volume overlaps of these Gla carboxylate oxygens with Ca are indicated in Table 4 for the two Ca^{2+}-bound structures.

Table 4
Geometrical characteristics of Gla-domain pockets

	Pocket volume, Å^3		Opening area, Å^2	
	C	D	C	D
Factor IX-Ca	111.4	193.4	24.5	62.8
Factor VII-Ca	88.3	15.6	27. 0	15.0
Prothrombin-Sr	114.4	18.9	38.4	22.3
Prothrombin-Ca	57.5	–	28.5	–

The volume of the C and D pockets and the area of the openings connecting the pocket concavities to the solvent spaces are measured using alpha-shape based software.

conclusions are derived from studies with factor X [17,18].

Results of experiments with added PSPC on either membrane system are consistent with previous kinetic studies indicating that substrate-lipid interaction precedes the catalytic step [15]. That the initial collisions of substrate with procoagulant membranes involve sites other than TF is also predictable from diffusional theory [37].

The effect of ionic strength was independent of bulk calcium concentration, within a millimolar range, consistent with high-affinity calcium interaction during the reaction. To investigate the possibility that this interaction involves exposed bound-calcium charges on the surface of the Gla-domain, we analyzed the pocket structure of factor IX and other homologous proteins. We use the alpha-shape method to identify and measure surface pockets analytically on the available Gla-domain structures [25].

A conserved structural motif observed in the Gla-domains is the presence of a pocket, found in calcium-bound factor IX, calcium-bound factor VII, calcium-bound prothrombin, and strontium-bound prothrombin. This pocket is in the same geometrical location on the various Gla-domains and consists of roughly the same or equivalent residues, after the sequences are aligned. The volume of this pocket ranges between 57 and 114 Å^3, large enough to accommodate additional calcium ions (about 22 Å^3). The area opening toward solvent spaces ranges between 24 and 38 Å^2. Based on the geometrical analysis of this conserved Gla-domain structure, we propose that the solvent-exposed surface of pocket C (as named in [18]) is a likely site, common among coagulation zymogens for calcium-mediated interactions with the membrane. This concave pocket may pro-

vide the necessary structural scaffold for extra calcium binding, which may, in turn, be responsible for the enhanced calcium affinity observed biochemically. For example, several of the atoms lining this pocket are carboxylate oxygens with low or no volume overlaps with calcium. These oxygen atoms may provide the coordinating partners for additional calcium. The site occupied by this pocket in the strontium-bound prothrombin has been proposed earlier as the membrane contact site [11]. Interestingly, some of the residues that contribute atoms to the pockets are from the region proposed as the hydrophobic binding site [19]. Together, these observations suggest that both electrostatic and hydrophobic reactivities may be contained within a relatively small region near the N-terminal loop of the Gla-domain.

The Gla-domain of factor IX is disordered in its calcium-free form but resolved when calcium is bound. The Gla-domain of prothrombin is disordered in free form and in magnesium-bound form and resolved in both calcium and strontium-bound forms [19]. These structural observations are consistent with previous biochemical studies, where strontium and calcium-bound prothrombin where shown to bind to phospholipids, and magnesium-bound prothrombin did not bind to phospholipids [39].

Table 5
Volume overlaps between calcium and Gla-carboxylate oxygens in pocket C

	OE4	OE3	OE2	OE1
Ca^{2+}-Factor VII				
CGU 29	3.2, 3.2	4.5, 3.6	0	1.3
CGU 16	0	3.6, 4.0	3.9	4.6, 3.6
CGU 7	4.2	0	4.4	2.7
Ca^{2+}–Prothombin				
CGU 30	3.7	3.5	0	4.2
CGU 17	1.6	5.8	2.6	3.5
CGU 8	2.8, 3.8	2.7	2.4	0

Values correspond to van der Waals volume overlaps between calcium and Gla carboxylate oxygens, expressed in Å^3, in the C pocket of factor VIIa and prothrombin fragment 1. These are the only two Gla-domain structures in which the calcium atoms are resolved. The overlaps with each calcium are listed separately. For example, CGU 29 of factor VIIa has volume overlaps of 4.5 and 3.6 Å^3 with calcium 3 and 9, respectively. (The calcium atoms are not identified in the table to simplify presentation.)

Based on reported analysis of the structures of prothrombin, most of the calcium atoms are not directly accessible to solvent and are therefore unlikely to participate in the formation of multiple ionic bridges with membrane, as initially proposed [12]. However, results from binding experiments indicate that there are more calcium atoms in the prothrombin/membrane complex than the seven atoms observed in the prothrombin fragment 1 structures [7,10]. Furthermore, the affinity of calcium for zymogen-membrane complexes and during functional reactions is higher than the affinity of free calcium for charged membranes. For zymogen binding and activation, half-saturating concentrations of calcium are in the 0.5–2 mM range whereas the association constant for purely electrostatic interaction between calcium and PSPC membranes is 12 M^{-1} [14]. The affinity of calcium for membrane–zymogen complexes is higher than would be expected from generic ionic interactions with phospholipids. Instead, these observations are more consistent with stereospecific interaction.

The structures of calcium-bound factors IX, VIIa, and strontium-bound prothrombin have an additional pocket also lined by atoms from Gla residues and residues from the proposed hydrophobic stack [8,9,19] (see the D pocket in Fig. 6B,D,E). This pocket may also participate in the functional binding of calcium with membrane, since it could accommodate either a more buried or a partially exposed calcium. However, this pocket is not seen in the calcium-bound prothrombin structure and in the other X-ray structures its volume is smaller than that of calcium. There are two additional pockets on the factor IX Gla-peptide NMR structure. These two pockets are not seen in any of the larger calcium-bound structures.

The value of effective charges measured during factor IX and X activation suggests one to two ionic contact sites. This value, determined from reaction rates, is not expected to coincide numerically with the actual number of charges carried by the reactants. Apart from the structural simplifications of electrostatic theory [36], the charge determined experimentally depends on the average number of ionic contacts during the reaction transient. During this transient, multiple rapid collisions can occur. Each collision may be stabilized by a different number of

ionic contacts [40]. For molecules with several pockets on the Gla-domain, the different spatial arrangements and orientations of pocket openings increase the probability of stabilized contacts between the membrane and the Gla-domain. The nonspecific and delocalized nature of ionic contacts improves both the efficiency of initial interaction and the chance of finding more specific docking orientations.

The experimentally measured effective charge and the identification of structural pocket motifs demonstrated in the present studies are consistent with a membrane–substrate bridging mechanism, involving both electrostatic and stereospecific calcium binding. The initial collisional contacts would be mediated by one or two asymmetrical calcium 'bridges'. The interaction of calcium with negative charges in the Gla-domain is stabilized by the pocket's concave shape. The initial interaction on the membrane side, on the other hand, is purely electrostatic (i.e., nonspecific and delocalized). This mechanism can explain both the calcium requirements and the observed lack of complete zymogen–membrane dissociation in the presence of excess calcium. This mechanism does not preclude subsequent hydrophobic interactions [8,9,17,41,42] or the possibility of additional ionic contacts involving charges outside the pockets.

Acknowledgements

References

[1] G.L. Nelsestuen, in: H. Sigal (Ed.), Metal Ions in Biological Systems, pp. 353–380 Marcel Dekker, New York, 1984.

[2] C. Vermeer, γ-Carboxyglutamate-containing proteins and the vitamin K-dependent carboxylase, Biochem. J. 266 (1990) 625–636.

[3] R.A. Schwalbe, J. Ryan, D.M. Stern, W. Kisiel, B. Dahlback, G.L. Nelsestuen, Protein structural requirements and properties of membrane binding by gamma-carboxyglutamic acid-containing plasma protein and peptides, J. Biol. Chem. 262 (1989) 20288–20296.

[4] M. Soriano-Garcia, K. Padmanabhan, A.M. de Vos, A. Tulinsky, The Ca^{2+} ion and membrane binding structure of the Gla domain of Ca-prothrombin fragment 1, Biochemistry 31 (1992) 25554–25566.

[5] S.J. Freedman, B.B. Furie, J.D. Baleja, Structure of the calcium ion-bound γ-carboxyglutamic acid-rich domain of factor IX, Biochemistry 34 (1995) 12126–12137.

[6] D.W. Banner, A. D'Arcy, C. Chene, F.K. Winkler, A. Guha, W.H. Konigsberg, Y. Nemerson, The crystal structure of the complex of blood coagulation factor VIIa with soluble tissue factor, Nature 380 (1996) 41–46.

[7] T.K. Lim, V.A.G. Bloomfield, G.L. Nelsestuen, Structure of the prothrombin-and blood clotting factor X-membrane complexes, Biochemistry 16 (1977) 4177–4181.

[8] M. Sunnerhagen, S. Forsen, A.-M. Hoffren, T. Drakenberh, O. Teleman, J. Stenflo, Structure of the Ca(2+)-free Gla domain sheds light on membrane binding of blood coagulation proteins, Nat. Struct. Biol. 6 (1995) 504–509.

[9] V. Koppaka, J. Wang, M. Banerjee, B.R. Lentz, Soluble phospholipids enhance factor Xa-catalyzed prothrombin activation in solution, Biochemistry 35 (1966) 7482–7491.

[10] D.W. Deerfield III, D.L. Olson, P.L. Berkowitz, P.A. Byrd, K.A. Koehlrt, L.G. Pedersen, R.G. Hiskey, Mg (II) Binding by bovine prothrombin fragment 1 via equilibrium dialysis and the relative role of Mg (II) and Ca (II) in blood coagulation, J. Biol. Chem. 262 (1987) 4017–4023.

[11] J.F. McDonald, A.M. Shah, R.A. Schwalb, W. Kisiel, B. Dahlback, G.L. Nelsestuen, Comparison of naturally occurring vitamin K-Dependent proteins: Correlation of amino acid sequences and membrane binding properties suggests a membrane contact site, Biochemistry 36 (1997) 5120–5127.

[12] G.L. Nelsestuen, W. Kisiel, G. Di Scipio, Interaction of vitamin K dependent proteins with membranes, Biochemistry 17 (1978) 2134–2138.

[13] G.L. Nelsestuen, T.K. Lim, Equilibria involved in prothrombin-and-blood clotting factor X-membrane binding, Biochemistry 16 (1977) 4164–4171.

[14] S. McLaughlin, N. Mulrine, T. Gresalfi, G. Vaio, A. McLaughlin, Adsorption of divalent cations to bilayer membranes containing phosphatydylserine, J. Gen. Physiol. 77 (1981) 445–473.

[15] S. Krishnaswamy, A.K. Field, T.S. Edgington, J.H. Morrissey, K.G.J. Mann, Role of the membrane surface in the activation of human coagulation factor X, Biol. Chem. 267 (1992) 26110–26120.

[16] L.V.M. Rao, S.I. Rapaport, Activation of factor VII bound to tissue factor: A key early step in the tissue factor pathway of blood coagulation, Proc. Natl. Acad. Sci. U.S.A. 85 (1988) 9503–9508.

[17] F. London, P.N. Walsh, The role of electrostatic interactions in the assembly of factor X activating complex on both activated platelets and negatively-charged phospholipid vesicles, Biochemistry 35 (1996) 12146–12154.

[18] M.P. McGee, H. Teuschler, J. Liang, Effective electrostatic charge of coagulation factor X in solution and on phospholipid membranes: implications for activation mechanisms and structure-function relationships of the Gla domain, Biochem. J. 330 (1998) 533–539.

[19] S.J. Freedman, M.D. Blostein, J.D. Baleja, M. Jacobs, B.C. Furie, B. Furie, Identification of the phospholipid binding site in the vitamin K-dependent blood coagulation protein Factor IX, J. Biol. Chem. 271 (1996) 16227–16236.

[20] V.K. La Mer, Reaction velocity in ionic systems, Chem. Rev. 10 (1930) 179–217.

[21] G.J. Scatchard, The rate of reaction in changing environments, Am. Chem. Soc. 52 (1930) 52–61.

[22] S. Glasstone, K.J. Laidler, H. Eyring, The Theory of Rate Processes, 1st ed., McGraw-Hill, New York, 1941.

[23] Y. Koutalos, T.G. Ebrey, H.R. Gilson, B. Honing, Octopus photoreceptor membranes surface charge density and pK of the Shiff base of the pigments, Biophys. J. 58 (1990) 496–501.

[24] H. Edelsbrunner, E. Mucke, Three-dimensional alpha shapes, ACM Trans. Graphics 13 (1994) 43–72.

[25] J. Liang, H. Edelsbrunner, C. Woodward, Anatomy of protein pockets and cavities: Measurement of binding site geometry and implications for binding design, Protein Sci. 7 (1998) 1884–1897.

[26] L. Van Lenten, G. Ashwell, Studies on the chemical enzymatic modification of Glycoproteins. A general method for the titration of sialic acid containing glycoproteins, J. Biol. Chem. 246 (1971) 1889–1894.

[27] N.L. Sanders, S.P. Bajaj, A. Zivelin, S.T. Rapaport, Inhibition of Tissue factor/factor VIIa in plasma requires factor X and an additional plasma component, Blood 66 (1985) 204–212.

[28] M. Zur, Y. Nemerson, Kinetics of factor IX activation via the extrinsic pathway. Dependence of Km on tissue factor, J. Biol. Chem. 255 (1980) 5703–5710.

[29] S.D. Carson, W.H. Konisber, Cadmium increases tissue factor coagulation (factor III) activity by facilitating its reassociation with lipids, Science 208 (1980) 307–309.

[30] T. Heimburg, D. Marsh, Thermodynamics of the interaction of proteins with lipid membranes, in: K. Mertz Jr., B. Roux (Eds.), Biological Membranes, Birhkhauser, Boston, 1966, pp. 405–414.

[31] F.J. Jahnig, Electrostatic free energy and shift of the phase transitions for charged lipid membranes, Biophys. Chem. 4 (1976) 309–318.

[32] J. Georg, I.M. Freeman, Theoretical Physics, Dover Publications, New York, 1958, pp. 263–292, 547–552..

[33] H. Trauble, M. Teubner, P. Woolley, H. Eibl, Electrostatic interactions at charged lipid membranes. I. Effects of pH and univalent cations on membrane structure, Biophys. Chem. 4 (1976) 319–342.

[34] H. Edelsbrunner, M. Facello, J. Liang, On the Definition and Construction of Pockets in Macromolecules, Proc. 1st Pacific Sym. Biocomp., World Scientific, Singapore, 1996.

[35] F.M. Richards, Areas, volume packing and protein structure, Annu. Rev. Biophys. Bioeng. 6 (1977) 151–176.

[36] S. McLaughlin, The electrostatic properties of membranes, Annu. Rev. Biophys. Chem. 18 (1989) 113–136.

[37] H.C. Berg, E.M. Purcell, Physics of chemoreception, Biophys. J. 20 (1977) 193–219.

[38] R.R. Sokal, F.J. Rohlf, Introduction to Biostatistics, W.H. Freeman, San Francisco, 1973.

[39] G.L. Nelsestuen, M. Broderius, G. Martin, Role of γ-carboxyglutamic acid. Cation specificity of prothrombin and factor X-phospholipid binding, J. Biol. Chem. 251 (1976) 6886–6893.

[40] S.H. Northup, J.O. Boles, C.L. Reynolds, Brownian dynamics of cytochrome c and cytochrome c peroxidase association, Science 241 (1988) 67–70.

[41] M. Borowski, B.C. Furie, S. Bauminger, B. Furie, Prothrombin requires two sequential metal-dependent conformational transitions to bind phospholipid, J. Biol. Chem. 262 (1986) 1469–14975.

[42] L. Zhang, F.J. Castellino, The binding energy of human coagulation protein C to acidic phospholipid vesicles contains a major contribution from leucine 5 in the γ-carboxyglutamic acid domain, J. Biol. Chem. 269 (1994) 3590–3595.